ACTRIIA-Fc rebalances activin/GDF versus BMP signaling in pulmonary hypertension

Lai-Ming Yung[1,*], **Peiran Yang**[1,*], **Sachindra Joshi**[2], **Zachary M. Augur**[1], **Stephanie S. J. Kim**[1], **Geoffrey A. Bocobo**[1], **Teresa Dinter**[1], **Luca Troncone**[1], **Po-Sheng Chen**[1,3], **Megan E. McNeil**[1], **Mark Southwood**[4], **Sergio Poli de Frias**[5], **John Knopf**[2], **Ivan O. Rosas**[5], **Dianne Sako**[2], **R. Scott Pearsall**[2], **John D. Quisel**[2], **Gang Li**[2], **Ravindra Kumar**[2], **Paul B. Yu**[1,†]

[1]Division of Cardiovascular Medicine, Department of Medicine, Brigham and Women's Hospital, Harvard Medical School, Boston, MA 02115, USA.

[2]Acceleron Pharma Inc., Cambridge, MA 02139, USA.

[3]Department of Internal Medicine, College of Medicine, National Cheng Kung University, Tainan City 704, Taiwan.

[4]Department of Pathology, Royal Papworth Hospital, Cambridge CB2 0AY, UK.

[5]Division of Pulmonary and Critical Care Medicine, Department of Medicine, Brigham and Women's Hospital, Harvard Medical School, Boston, MA 02115, USA.

Abstract

Human genetics, biomarker, and animal studies implicate loss of function in bone morphogenetic protein (BMP) signaling and maladaptive transforming growth factor–β (TGFβ) signaling as drivers of pulmonary arterial hypertension (PAH). Although sharing common receptors and effectors with BMP/TGFβ, the function of activin and growth and differentiation factor (GDF) ligands in PAH are less well defined. Increased expression of GDF8, GDF11, and activin A was detected in lung lesions from humans with PAH and experimental rodent models of pulmonary hypertension (PH). ACTRIIA-Fc, a potent GDF8/11 and activin ligand trap, was used to test the roles of these ligands in animal and cellular models of PH. By blocking GDF8/11- and activin-mediated SMAD2/3 activation in vascular cells, ACTRIIA-Fc attenuated proliferation of pulmonary arterial smooth muscle cells and pulmonary microvascular endothelial cells. In several experimental models of PH, prophylactic administration of ACTRIIA-Fc markedly improved hemodynamics, right ventricular (RV) hypertrophy, RV function, and arteriolar remodeling. When

administered after the establishment of hemodynamically severe PH in a vasculoproliferative model, ACTRIIA-Fc was more effective than vasodilator in attenuating PH and arteriolar remodeling. Potent antiremodeling effects of ACTRIIA-Fc were associated with inhibition of SMAD2/3 activation and downstream transcriptional activity, inhibition of proliferation, and enhancement of apoptosis in the vascular wall. ACTRIIA-Fc reveals an unexpectedly prominent role of GDF8, GDF11, and activin as drivers of pulmonary vascular disease and represents a therapeutic strategy for restoring the balance between SMAD1/5/9 and SMAD2/3 signaling in PAH.

INTRODUCTION

Pulmonary arterial hypertension (PAH), defined as precapillary pulmonary hypertension (PH) with mean pulmonary arterial pressure (mPAP) of >20 mmHg in the presence of normal pulmonary capillary wedge pressure of 15 mmHg and an elevated pulmonary vascular resistance of >3.0 Wood units (1), is a debilitating disease of progressive loss of the pulmonary circulation, with slightly better than 50% survival at 5 years after diagnosis (2). In contrast to currently approved vasodilator therapies, novel therapies targeting underlying mechanisms of vessel remodeling could yield improved outcomes. We hypothesized that an imbalance of activin and growth and differentiation factor (GDF) versus bone morphogenetic protein (BMP) signaling could be corrected therapeutically to mitigate pulmonary vascular remodeling. The identification of loss-of-function mutations in the BMP type 2 receptor (*BMPR2*), its co-receptors *ACVRL1* and *ENG*, its ligand BMP9/*GDF2,* and effectors *SMAD4* and *SMAD9* in heritable forms of PAH (HPAH) (3, 4) has implicated deficient BMP signaling in PAH. Lung tissues from human PAH and experimental PH exhibit diminished BMPRII expression and BMP signaling in the presence or absence of *BMPR2* loss-of-function mutations (5–9), supporting a protective role of BMP signaling in non-heritable forms of PAH and nongenetic models of PH. Also consistent with a protective role of BMP signaling, exogenous BMP9 rescues PH in multiple animal models (10), whereas BMP9 ligand trap activin receptor–like kinase 1–Fc (ALK1-Fc) exacerbates hypoxia-induced PH (11). Elevated transforming growth factor–β (TGFβ) expression and signaling activity are found in human PAH and multiple experimental PH models (8, 12–16), and inhibitors of ALK4/5/7 and a selective TGFβ1/3 ligand trap (TGFBRII-Fc) ameliorate experimental PH (5, 8, 12, 17), consistent with a pathogenetic role of excess TGFβ signaling.

Although activin and GDF ligands share receptors in common with BMP and TGFβ and preferentially activate TGFβ effectors SMAD2 and SMAD3, their status as therapeutic targets in PAH is less clear. It was previously reported that activin A is increased in the circulation of human PAH, is overexpressed in the lungs of mice with hypoxia- induced PH, and promotes proliferation and vasoactive gene expression in pulmonary artery smooth muscle cells (PASMCs) (18). Consistent with this proproliferative effect, another study demonstrated that activin A neutralizing antibodies inhibit PASMC growth in basal media (19). Treatment of cultured rat PASMCs with monocrotaline (MCT) pyrrole enhances expression of ACTRIIA, the principal type 2 receptor for activin and GDF ligands, while diminishing expression of BMPR2, suggesting a reciprocal relationship between BMP and

activin signaling in PH (20). These studies suggest a broader pattern of imbalanced BMP versus TGFβ and activin/GDF signaling in PAH; however, the role of activin and GDF as therapeutic targets in PAH has yet to be established.

To test the pathogenetic contribution of activin and GDF ligands in experimental PH, we used the activin and GDF ligand trap ACTRIIA-Fc, a homodimer of type II activin receptor ACTRIIA extracellular domains expressed as an immunoglobulin G (IgG) Fc domain fusion protein. Sotatercept, a recombinant human ACTRIIA IgG1 Fc fusion protein, has been tested in phase 2 studies for anemia and multiple myeloma (21). A murine ACTRIIA-Fc cognate known as RAP-011 has been generated and used in rodent studies (22). ACTRIIA-Fc potently binds activin A/B and GDF8/11, which preferentially activate SMAD2/3 via ACTRIIA or ACTRIIB in combination with type 1 receptors ALK4, ALK5, or ALK7. We hypothesized that sequestering these ligands could abrogate their direct contributions to pulmonary vascular remodeling or restore a favorable balance of BMP versus TGFβ/ activin/GDF signaling.

RESULTS

ACTRIIA ligand expression is increased in the pulmonary vasculature of PH and PAH

Immunohistochemistry of lung tissues revealed enhanced expression of activin A, GDF8, and, to a lesser extent, GDF11 in the distal pulmonary arterioles of patients with idiopathic PAH (IPAH) and *BMPR2* mutation–positive HPAH versus healthy controls, as well as vessels from MCT-exposed and SUGEN5416 and hypoxia [SU-Hx; FiO_2 (fraction of inspired oxygen) = 0.10]–exposed rats with PH versus controls (Fig. 1). Activin A was expressed in the vascular lesions of six of seven PAH lungs, and GDF8 was expressed in seven of eight PAH lungs, whereas GDF11 showed more sporadic expression in four of seven PAH lungs (fig. S1). Costaining with antibodies against α-smooth muscle actin (α-SMA) revealed expression of activin A in the intima and media of obstructive and plexiform lesions in human PAH and in the media of MCT- and SU-Hx–treated rat vessels, whereas GDF8 and GDF11 were expressed in the intima and media of diseased vessels in both human and rat lungs. Elevated activin A was detected in serum from patients with World Health Organization (WHO) Group 1 PAH but not Group 2 or Group 3 PH (fig. S2).

ACTRIIA ligands activate SMAD1/5/9 and SMAD2/3 signaling with enhanced proproliferative and diminished proapoptotic effects in PAH-derived endothelial cells

On the basis of these patterns of expression, the signaling and function of activin and GDF ligands were tested in human pulmonary microvascular endothelial cells (PMVECs) and PASMCs. Western blot analysis demonstrated that GDF8, GDF11, activin A, and activin B induced SMAD2/3 phosphorylation in PMVECs isolated from healthy control and PAH donors (Fig. 2A and fig. S3). GDF11 and activin A modestly activated SMAD1/5/9 but were much less potent than BMP9. ACTRIIA-Fc blocked the activation of SMAD2/3 and SMAD1/5/9 by activin and GDF ligands but not BMP9. When exposed to BMP9 at concentrations up to its median effective concentration (EC_{50}), cotreatment with ACTRIIA-Fc enhanced BMP-responsive element transcriptional reporter (BRE-Luc) activity in telomerase immortalized human microvascular endothelial (TIME) cells (Fig. 2B) and

similarly enhanced activation of SMAD1/5/9 in human PMVECs (Fig. 2C) and bovine aortic endothelial cells (fig. S4A).

We investigated potential competition of these ligands with BMP9 signaling by cotreating TIME cells with BMP9 and these ligands, revealing attenuation of BMP9-mediated transcriptional activity by activin A, GDF8, and GDF11 (Fig. 2D). The inhibition of BMP9 activity by GDF11 could be reversed by cotreatment with ACTRIIA-Fc (Fig. 2E). Similarly, inhibition of BMP9-induced SMAD1/5/9 activation or *ID1* mRNA transcription by GDF11 was normalized by treatment with ACTRIIA-Fc in human PMVECs (fig. S4B) and pulmonary artery endothelial cells (PAECs) (fig. S4C). In PMVECs from control and PAH donors, BMP9 stimulated proliferation in a manner not affected by ACTRIIA-Fc (Fig. 2, F and G), as analyzed by ^{3}H-thymidine incorporation. Although activin A and GDF11 had no effect or modestly inhibited proliferation, respectively, in control PMVECs, both of these ligands stimulated proliferation in HPAH-derived PMVECs. The proliferation of PMVECs from control and PAH donors when cultured in the presence of activin A or GDF11 was inhibited by ACTRIIA-Fc to varying degrees. In control PMVECs, activin A and GDF11, but not BMP9, increased apoptosis (fig. S5). None of these ligands affected the apoptosis of PAH-derived PMVECs, which exhibited significantly decreased rates of apoptosis compared to control cells under basal conditions ($P = 0.003$). In a tube formation assay, basic fibroblast growth factor (bFGF) increased total branch length in control PMVECs, whereas BMP9, activin A, and GDF11 had minimal effect, and none of these cytokines had significant impact on PAH-derived PMVECs (fig. S6). Together, these findings showed that activin A and GDF11 enhanced the growth of PAH-derived PMVECs, whereas GDF11 inhibited growth and activin A promoted apoptosis in control-derived PMVECs.

ACTRIIA ligands activate SMAD1/5/9 and SMAD2/3 signaling in pulmonary arterial smooth muscle to modulate myogenic and fibrogenic gene expression

In healthy control or PAH-derived PASMCs, treatment with TGFβ1, GDF8, GDF11, and activin A induced phosphorylation of SMAD1/5/9 and SMAD2/3 to varying degrees, whereas cotreatment with ACTRIIA-Fc abrogated signaling of all ligands but TGFβ1 (Fig. 2H and fig. S7). GDF8, GDF11, activin A, and activin B up-regulated mRNA and protein expression of myogenic genes α-SMA and calponin in a manner reminiscent of TGFβ1 but, unlike TGFβ1, were blocked by ACTRIIA-Fc (Fig. 2, I to L, and fig. S8, A and B). These observations suggested that these ligands promote phenotypic modulation of smooth muscle contractile genes similarly to TGFβ1; however, various smooth muscle phenotypic genes regulated by TGFβ1 were differentially regulated by GDF8, GDF11, and activin A (fig. S8C). Treatment with platelet-derived growth factor–BB (PDGF-BB), but not complete media, induced proliferation of PASMCs in a manner that was inhibited by ACTRIIA-Fc, whereas GDF11 and activin A had modest proproliferative effects in control PASMCs (Fig. 2M and fig. S9A). In PAH-derived PASMCs, neither activin A nor GDF11 induced proliferation; however, growth of PAH-derived PASMCs in the presence of exogenous activin A was inhibited by ACTRIIA-Fc (fig. S9, B and C). Neither activin A nor GDF11 significantly affected apoptosis in control or PAH PASMCs; however, basal rates of apoptosis appeared to be lower in diseased versus healthy cells (fig. S9, D to F). In addition, none of the tested BMP, GDF, or activin ligands significantly affected migration of healthy

control or PAH-derived PASMCs in a scratch assay (fig. S10). These findings were replicated in a minimum of three distinct control and three PAH donor-derived PASMC cultures.

Impact of ACTRIIA-Fc in MCT-induced experimental PH

Given the effects of ACTRIIA-Fc in antagonizing GDF8/11- and activin A/B–mediated signaling in PASMCs, enhancing BMP9 signaling in PMVECs, and blocking the proproliferative effects of GDF11 and activin A in PMVECs and PASMCs, we hypothesized that ACTRIIA-Fc might exert therapeutic antiremodeling effects in experimental PH via its impact on these cells. ACTRIIA-Fc was tested prophylactically in the MCT rat model of PH, known to exhibit impaired BMPR2-SMAD1/5/9 and enhanced SMAD2/3 signaling (17). ACTRIIA-Fc [15 mg/kg, twice weekly, subcutaneously (sc)] normalized mPAP (19.9 ± 1.2 mmHg versus 46.2 ± 2.4 mmHg; $P < 0.0001$), right ventricular hypertrophy (RVH; 0.29 ± 0.04 versus 0.55 ± 0.04; $P < 0.001$), and pulmonary arteriolar muscularization as compared with vehicle-treated rats (Fig. 3, A to F, and fig. S11). There was no effect on systemic arterial pressures. Sildenafil (30 mg/kg, twice daily, orally), a phosphodiesterase 5 inhibitor approved for the treatment of PAH that functions as a vasodilator, had more modest effects on hemodynamics and did not improve remodeling.

Delayed treatment with ACTRIIA-Fc [1, 3, or 10 mg/kg, intraperitoneally (ip), twice weekly] 4 weeks after MCT administration, a time point at which PH was established in rats, potently reduced PH at all doses (Fig. 3, G and H) and reduced RVH and attenuated pulmonary arteriolar muscularization at the two higher doses (Fig. 3, I to L). Consistent with its antiproliferative effects in vitro, ACTRIIA-Fc (10 mg/kg) reduced the number of Ki67-positive cells in MCT lungs (Fig. 3M and fig. S12A). Similar to its impact on SMAD2/3 signaling in vitro, ACTRIIA-Fc normalized the activation of SMAD2 seen in lung lysates of MCT-treated rats by Western blot (Fig. 3, N and O). No significant impact of ACTRIIA-Fc on activation of SMAD1/5/9 or apoptosis in whole-lung tissues was observed in this model (fig. S12, B and C).

Impact of ACTRIIA-Fc in SU-Hx–induced experimental PH

In SU-Hx rats, a vasculoproliferative model known to develop progressive obliterative and complex lesions reminiscent of severe human disease (23), prophylactic treatment with ACTRIIA-Fc (15 mg/kg, sc, twice weekly) over 4 weeks of exposure to SU-Hx normalized mPAP (21.1 ± 1.1 versus 43.3 ± 2.4 mmHg; $P < 0.0001$), RVH (0.28 ± 0.01 versus 0.61 ± 0.02; $P < 0.0001$), and arteriolar muscularization compared to vehicle-treated SU-Hx rats, without affecting systemic arterial pressures (Fig. 4, A to F, and fig. S13, A to C). In contrast, sildenafil (60 mg/kg, twice daily, orally) modestly reduced mPAP (33.6 ± 2.0 mmHg; $P < 0.01$) without affecting RVH or the frequency of muscularized vessels. When ACTRIIA-Fc was administered (1, 3, or 10 mg/kg, ip, twice weekly) after 3 weeks of SU-Hx, a time point at which moderate PH was established, RV systolic pressure (RVSP), RVH, arteriolar wall thickness, and vessel muscularization were reduced at the highest dose (Fig. 4, G to L). Consistent with its antiproliferative activity in vitro, ACTRIIA-Fc reduced the number of Ki67-positive cells in vessels and perivascular tissues of SU-Hx–exposed rats (Fig. 4M and fig. S13D). Elevated mRNA expression of SMAD2/3 target gene *Pai-1*

observed in SU-Hx lungs was attenuated by ACTRIIA-Fc but without corresponding changes in whole-tissue phosphorylated SMAD2 (Fig. 4N and fig. S14).

To test the efficacy in a model of severe obliterative PH, rats were allowed to progress for 5 weeks after exposure to SU-Hx before starting treatment (Fig. 4, O to T). After 5 weeks, rats had developed severe PH approaching systemic pressures, severe RVH, and obliterative vasculopathy that persisted through 9 weeks. Treatment with ACTRIIA-Fc (5 mg/kg, sc, twice weekly) from weeks 6 to 9 after SUGEN5416 exposure reversed existing PH and RVH, effects not seen with sildenafil treatment. Moreover, ACTRIIA-Fc reduced the proportion of occluded vessels, medial hypertrophy, and wall thickening. Treatment with ACTRIIA-Fc, but not vasodilator, normalized echocardiographic measures of PH and RV dysfunction (fig. S15, A to D). ACTRIIA-Fc did not alter arteriolar muscularization, cardiac output, or systemic pressure in this model (Fig. 4U and fig. S15, E to H). The frequencies of TUNEL$^+$ (terminal deoxynucleotidyl transferase–mediated deoxyuridine triphosphate nick end labeling–positive) apoptotic vascular cells in SU-Hx–exposed rat vessels at 5 and 9 weeks were 12 and 17%, respectively, whereas treatment with ACTRIIA-Fc increased the frequency of TUNEL$^+$ intimal cells to 34% at 9 weeks (Fig. 4V and fig. S16). In this severe SU-Hx model, treatment with ACTRIIA-Fc reduced the number of cells expressing phosphorylated SMAD2/3, abrogated *Pai-1* and *Inhba* mRNA expression in diseased lung tissues, and attenuated mRNA expression of E-selectin and P-selectin (Fig. 4W and figs. S17 and S18). No measurable impact of chronic ACTRIIA-Fc administration on serum hemoglobin (Hb) or hematocrit was seen in this rat study (fig. S19).

DISCUSSION

The current study extends the paradigm of dysregulated BMP and TGFβ signaling to implicate several activin and GDF ligands as key pathogenic drivers of PAH. GDF8/11 and activin A were overexpressed in diseased pulmonary vessels of human PAH and experimental PH and modulated the growth and phenotypic plasticity of vascular cells. ACTRIIA-Fc inhibited GDF8/11- and activin-mediated proliferation of smooth muscle cells and abrogated the ability of these ligands to induce proliferation and compete with surface receptors for BMP9 signaling in microvascular endothelial cells. In the lung tissues of experimental PH, ACTRIIA-Fc inhibited SMAD2/3 activation and *Pai-1* transcription, attenuated medial hypertrophy, inhibited cell proliferation, and promoted apoptosis in diseased vessels. Together, ACTRIIA-Fc inhibits pathophysiologic remodeling effects of activin and GDF signaling in the pulmonary vasculature and defines the contribution of these ligands to the paradigm of imbalanced SMAD1/5/9 versus SMAD2/3 signaling in PAH.

Beyond demonstrating efficacy in prophylactic and therapeutic MCT-induced and SU-Hx–induced models, ACTRIIA-Fc reverse- established obliterative vasculopathy accompanying severe PH and RV dysfunction in a 9-week SU-Hx rat model, suggesting that treatment might restore vessel patency in addition to preventing tissue remodeling. The antiremodeling effects of ACTRIIA-Fc may be related to its inhibition of proliferation seen in distinct PH models or its ability to increase apoptosis, which was diminished in diseased pulmonary vessels. Resensitizing vascular cells to proapoptotic stimuli may be a critical property of

effective antiremodeling strategies. Previous studies with imatinib, a tyrosine kinase inhibitor, showed potent antiremodeling effects in experimental PH in association with increased apoptosis (24), an effect that might be critical to its clinical efficacy in PAH (25, 26).

The impact of ACTRIIA-Fc on BMP9 signaling in endothelial cells might result from competition between GDF8/11, activin A/B, and BMP9 for shared type II receptors. BMPR2, ACTRIIA, and ACTRIIB are reported to bind and transduce BMP9 signals (7, 27, 28). ACTRIIB exhibits the highest affinity for BMP9: BMPR2 has 30-fold lower affinity, and ACTRIIA has ~300-fold lower affinity with a much faster dissociation rate (28). Sequestration of activin and GDF ligands by soluble ACTRIIA-Fc in the context of its relatively low affinity for BMP9 may increase the availability of membrane type II receptors for transducing BMP9. Our finding that ACTRIIA-Fc enhances BMP9 signaling in several endothelial cell types suggests an endogenous inhibitory function of some of these ligands, particularly GDF11, and is consistent with previous studies suggesting that competition between various BMP/TGFβ/activin ligands and their receptors appears to regulate signaling (29–31). Although treatment with ACTRIIA-Fc did not increase expression of *p*-SMAD1/5/9 in whole-lung tissues of experimental PH, this effect might be restricted to the vascular endothelium of treated tissues or it could be offset by inhibition of GDF8/11- or activin A/B–mediated activation of SMAD1/5/9. Consistent with antimyofibrogenic effects of treatment, whole-lung tissues from SU-Hx rats exhibited a dose-dependent decrease in the expression of *Pai-1* mRNA with ACTRIIA-Fc.

GDF8/11 and activin transduced SMAD2/3 activation and downstream transcriptional responses, but the impact of these ligands was not equivalent to the effects of TGFβ. A previous study highlighted the possible role of GDF11 in PAH, describing proproliferative, promigratory, and proangiogenic effects in PAECs, and relative protection from experimental PH in GDF11 knockout mice (32). The current study extends these potential roles to GDF8, GDF11, activin A, and activin B in both vascular smooth muscle and endothelium. In addition to being overexpressed in the remodeled vessels of experimental PH and human PAH, activin A was elevated in circulation of individuals with Group 1 PAH, recalling a prior study in which elevated circulating activin A was correlated with mortality in PAH (18). GDF8 is highly homologous to GDF11 (~90%) (33) and overlaps in function with GDF11 and activin A in regulating muscle mass and myocyte hypertrophy based on genetic loss-of-function and pharmacologic experiments (34, 35). Targeting GDF8, GDF11, and activin ligands as a group versus individually has proven to be more effective for increasing muscle mass (36–38). By analogy, it is likely that this set of ligands of ACTRIIA may have overlapping roles in pulmonary vascular disease. Similar to what was found in neuromuscular disease, a multiligand trap that binds this group of ligands may achieve greater efficacy in PAH than neutralizing individual ligands.

The activin/GDF ligand trap ACTRIIA-Fc achieves antiremodeling effects in pulmonary vascular disease that may be consistent with rebalancing of SMAD1/5/9 versus SMAD2/3 signaling in vascular cells, reversing hemodynamic, molecular, and histologic findings in multiple models of PH including severe vasculoproliferative disease. These effects are not seen with standard-of-care vasodilator therapy and may be related to the ability of

ACTRIIA-Fc to alter the balance between proliferation and apoptosis in vascular cells. The human analog sotatercept has been tested clinically for the treatment of anemia and multiple myeloma and was well tolerated in phase 1 and 2 studies involving more than 400 patients across 13 trials (21, 39, 40), with favorable pharmacokinetics and 3- to 4-week dosing in human subjects (21). The lowest effective doses of 1 to 3 mg/kg (sc) twice weekly tested in rats in the current study achieve exposures that are comparable to therapeutic and well-tolerated doses of 0.3, 0.7, and 1.5 mg/kg (sc) every 3 weeks in human studies. The extensive clinical experience and safety record with this agent have provided an opportunity for rapid translation as a nonvasodilator antiremodeling therapy for PAH, as pursued in the PULSAR (NCT03496207) and SPECTRA (NCT03496207) phase 2 clinical trials.

Our ability to predict the value of disease target and therapeutic agent is limited by the quality of the histopathology, tissue-derived cells, and animal models. The vascular cells cultured from PH and non-PH lungs retain some of their signaling and functional phenotypes but exhibit heterogeneity and lose contextual cues regulating growth and identity after dissociation and expansion outside of their normal niches. To limit heterogeneity, sampling error, and culture-induced artifacts, we used a panel of cells, lung tissues, and plasma derived from diverse patient and control donors and have qualified ACTRIIA ligand–related phenotypes on the basis of their consistency or being unique to disease-derived or control cells. As an approximation of PAH, MCT-induced PH in rats features medial hypertrophy and hemodynamically moderate PH but does not recapitulate the histopathological spectrum of human disease, lacking neointimal proliferative lesions and obstructive vasculopathy. MCT-induced PH may be responsive to vasodilators or agents that inhibit arteriolar muscularization but does not model the occlusive arteriopathy accompanying severe PAH. SU-Hx–induced PH can exhibit severe PH with vasculoproliferative and obliterative remodeling reminiscent of human disease, but because it is a progressive model, any delayed intervention is necessarily therapeutic and prophylactic. Both models develop in a short time frame and may not model chronic changes present in longstanding disease of years or decades in humans. We tested ACTRIIA-Fc prophylactically and in as delayed a fashion as possible while permitting animals to survive for analysis in these complementary models. To ensure reproducibility, these studies were corroborated by several independent operators, demonstrating dose-efficacy relationships in models of varying hemodynamic and histopathological severity. The proproliferative effects of ACTRIIA ligands found to be enhanced in PAH-derived PMVECs and the resistance to apoptosis in PAH-derived PMVECs and PASMCs appeared to be countered by the antiproliferative and proapoptotic effects of ACTRIIA-Fc in PH models; it is proposed that these specific effects could be the best predictors of efficacy for an antiremodeling agent for PAH. During the revision of this manuscript, preliminary results of the PULSAR trial were revealed, with sotatercept showing efficacy in the primary end point of improved pulmonary vascular resistance versus placebo at 24 weeks, as well as several secondary end points including improved 6-min walk distance and WHO functional class. The current data are presented as the preclinical rationale for the clinical study and to provide a mechanistic framework for understanding the impact of sotatercept as an antiremodeling drug for PAH.

Although the lower doses of 1 and 3 mg/kg twice weekly in these PH models overlap with the doses of 0.3 and 0.7 mg/kg every 3 weeks tested in PULSAR, it is unclear whether the

full potency of this strategy seen at higher doses in the PH models is replicated at the relative lower equivalent doses in humans and may leave an opportunity for testing higher doses in the future. On the other hand, although well tolerated, sotatercept is a potent therapy for anemia and can augment Hb and erythrocyte counts sufficiently to cause polycythemia in individuals with normal concentrations of Hb and is contraindicated in polycythemic individuals (41). These limitations, based on previous clinical experience, have been considered in the design of the PULSAR trial, with provisions to exclude individuals with Hb >16 at entry and to limit dosing for individuals with Hb >18 during the course of the study. In our study, the proerythrocytic effects of ACTRIIA-Fc were modest, which could have been limited by either the disease process or the model organism. By the same token, any potential benefit gained by correcting anemia, which is known to affect a portion of patients with PAH (42, 43), would not have been captured in our studies.

In summary, the GDF and activin ligand trap ACTRIIA-Fc exhibited consistent efficacy in several complementary animal models of PH, with antiproliferative and proapoptotic effects seen in the lung tissues of treated animals that were concordant with effects on vascular cells derived from human lungs affected by PAH. Despite the diverse physiologic functions of these ligands, previous clinical experience with the human analog sotatercept provided sufficient safety and dosing guidance to permit rapid translation of this concept, such that a clinical trial could be enrolled and completed in a contemporaneous fashion with the preclinical study. These studies show that repositioning can be a robust strategy for accelerating drug development and present several potential preclinical metrics for assessing the efficacy of a novel antiremodeling therapy, while revealing GDF and activin ligands to be critical drivers in the pathophysiology of PAH.

METHODS AND MATERIALS

Study design

The objective of this study was to investigate the impact of ligand trap ACTRIIA-Fc and its targeted ligands (GDF8, GDF11, activin A, and activin B) on pulmonary vascular biology and PH. For in vivo studies, the impact of test agent ACTRIIA-Fc on pulmonary pressures (RVSP or PA mean) in animal models of PH was considered a primary end point, with impact on RVH and pulmonary arteriolar remodeling considered secondary end points. All animals were segregated into treatment and control groups randomly, and all hemodynamic, physiologic, and histologic measurements were performed in a blinded manner with respect to treatment. Three separate operators at three separate sites performed hemodynamic measurements for independent replication. In some experiments, hemodynamic measurements were performed by direct PA cannulation, whereas in other experiments, the RV was cannulated, depending on which of three independent operators were responsible. On the basis of a hypothesized 30% absolute decrease in RV or PA pressures with ACTRIIA-Fc treatment versus vehicle and a percent coefficient of variation (%CV) of 25% based on previous studies, experimental groups of six animals would be 80% powered to detect this difference, whereas treatment groups of nine animals would be 90% powered to detect this difference. Thus, all animal studies were designed to include groups of 6 to 10 animals at the outset. At the conclusion of each animal study, hemodynamic data were not

obtained in some cases because of premature mortality or was excluded from analysis because of prespecified low heart rate threshold (<350 beats/min) during catheterization suggesting a moribund state. Fulton's index was reported for all animals without exception. Histologic data were obtained by sampling formalin-fixed paraffin-embedded sections from the right middle lobe of the lung or frozen sections from the right lower lobe of the lung after perfusion and fixation. A minimum of 30 to 50 small pulmonary arterioles from each animal subject were photographed and scored in a blinded fashion by two independent observers. Histologic measurements were presented as the mean and SD of measurements across all animals in each cohort and reported without exclusion. For in vitro studies, we hypothesized that ACTRIIA-Fc or its targeted ligands would affect a given end point by a minimum of 30%, with a %CV of 15%. Experimental groups consisting of three biological replicates would be 80% powered to this difference, whereas four replicates would be 90% powered to detect this difference. Thus, in vitro studies were designed to include groups of 3 to 10 biological replicates at the outset of each experiment. In some experiments that measured data from cells cultured in multiwell plates, high and low measurements were excluded from all experimental conditions to minimize variability due to differential growth of cells in centers versus edges of plate (plate effect). Raw data are provided in data files S1 and S2. All animal studies were performed under an approved protocol with oversight from the Brigham and Women's Hospital Institutional Animal Care and Use Committee. All human samples and clinical data were obtained with informed consent under an approved protocol with oversight from the Partners HealthCare Institutional Review Board.

Reagents

Recombinant ACTRIIA was expressed as a fusion protein with IgG Fc domain (ACTRIIA-Fc) in Chinese hamster ovary cells [(American Type Culture Collection (ATCC)] and purified with two rounds of affinity column chromatography, similar to previously described (44). Recombinant human TGFβ1, activin A, activin B, GDF8, GDF11, BMP9, and BMP4 were purchased from R&D Systems. Recombinant human VEGF and bFGF were purchased from PeproTech.

Serum ligand expression measurements in control and PAH patient serum

Enzyme-linked immunosorbent assay (ELISA) assays for human serum activin A and GDF11 were performed using Quantikine and DuoSet ELISA kits (catalog nos. DAC00B and DY1958–05, R&D Systems) according to the manufacturer's instructions and were validated for lack of cross-reactivity for homologous proteins (activin B and GDF8). Measurement of GDF8 in human serum was performed using a monospecific anti-human GDF8 antibody lacking cross-reactivity with GDF11 on a multiplex ELISA system (Meso Scale Discovery) using the standard manufacturer's protocol. Demographic and clinical characteristics of the serum donors are described in table S1.

Experimental PH models

Adult male Sprague-Dawley rats (6 to 10 weeks old but uniform within a given experiment; 150 to 170 g, 200 to 250 g, or 400 to 450 g, depending on the cohort) were purchased from Charles River Laboratories. Experimental protocols were approved by the Harvard Institutional Animal Care and Use Committee. Animals were housed at 24°C in a 12-hour

light/12-hour dark cycle where food and water were accessible ad libitum. PH was induced by administration of MCT (Oakwood Chemical; 40 mg/kg, sc) followed by 4 to 6 weeks of normoxia; or via administration of vascular endothelial growth factor receptor 1/2 (VEGFR1/2) receptor antagonist SUGEN5416 (APExBIO; 20 mg/kg, sc) followed by 3 weeks of normobaric hypoxia ($FiO_2 = 0.10$) and followed by 3 or 6 weeks of normoxia; or, alternatively, by SUGEN5416 (200 mg/kg, sc) followed by 4 weeks of hypoxia. Mortality and total number of animals examined in this study are summarized in table S2.

Invasive hemodynamic measurements and tissue isolation

Rats were anesthetized with isoflurane (2.5% induction, 0.5 to 1.5% maintenance), and RV pressures were measured by a minimally invasive closed chest approach using a curved tip 2 French pressure transducer catheter (Millar, SPR-513) inserted into the RV through the right internal jugular vein. To assess the degree of RVH, the RV free wall was dissected from the left ventricle plus septum (LV + S) in explanted hearts and weighed. The degree of RVH was determined from the ratio RV/(LV + S). Lungs were perfused with phosphate-buffered saline (PBS) via the RV to exclude circulating blood cells from the pulmonary circulation, and the right lower lung lobe was ligated, resected, and snap-frozen en bloc for analyses of RNA and protein expression. The pulmonary vasculature was perfused in situ via the RV with 1% paraformaldehyde (PFA) in PBS at 100 cm H_2O pressure for 1 min, followed by perfusion of the airways via the trachea at 20 cm H_2O for 1 min. Hb and hematocrit were measured using a HemaTrue blood analyzer (Heska) using 100 μl of heparinized blood samples collected by cardiac puncture.

Echocardiography in rat model of PH

Echocardiography was performed using VisualSonics small animal 20-MHz ultrasound probe applied to the anterior chest wall with animals in supine position. Anesthesia was induced using 2.5% isoflurane and maintained with 1.5% isoflurane throughout the study. RV wall thickness was assessed using M mode from the left parasternal view and measured at end diastole. Pulse-wave Doppler across the pulmonary valve in short-axis view at the level of the aortic valve was used to measure PA acceleration time, which served as a noninvasive surrogate measure of PA systolic pressure. Tricuspid annular plane systolic excursion measured from the lateral tricuspid valve annulus was used to assess RV function. Analysis of obtained images was performed using Vevo 2100 software package (VisualSonics).

Lung histomorphometry and immunohistochemistry

To determine the degree of pulmonary vascular remodeling, lungs were embedded for paraffin sectioning or optimal cutting temperature compound sectioning (8 μm) and slides were stained with α-SMA and von Willebrand factor as described previously (11). Muscularization of distal intra-acinar vessels (diameter, 10 to 50 μm; 20 to 30 vessels per sample) was scored in a blinded fashion and categorized as either nonmuscular, partially muscularized, or fully muscularized, and relative proportions were expressed as a percentage of total vessels. For fully muscularized intra-acinar vessels, medial wall thickness was calculated on the basis of the following formula: medial thickness − (external diameter − internal diameter)/external diameter × 100. To determine the frequency of proliferating cells

in rat models of PH, lung tissue sections were stained with a Ki67-specific rabbit monoclonal antibody (Cell Signaling Technology, no. 9129), followed by horseradish peroxidase (HRP)–conjugated anti-rabbit IgG. Slides were developed with ImmPACT DAB peroxidase (HRP) substrate (Vector Laboratories) and counterstained with hematoxylin. The number of Ki67-positive cells was counted in a blinded fashion in 10 to 20 randomly chosen high-powered fields. Immunohistochemical staining using activin A, GDF8, and GDF11 primary antibodies was followed by HRP-conjugated secondary and developed with ImmPACT DAB peroxidase (HRP) substrate. These slides were costained with alkaline phosphatase (AP)–conjugated α-SMA and developed with Vector Blue AP Substrate. The specificity of each antibody used for immunohistochemical staining was determined by staining samples with only the secondary antibody for both rat and human tissues. Immunohistochemistry staining of pSmad2/3 on formalin-fixed, paraffin-embedded lung sections was performed using polyclonal rabbit anti-pSmad2/3 antibody (ab63399, Abcam) using the Leica BOND RX automated advanced staining system, according to Leica immunohistochemistry protocol F. Antibodies used in this study are listed in table S3.

Gene expression studies

Frozen lung samples were homogenized, and total RNA was extracted using TRIzol reagent. Reverse transcription (RT) and quantitative polymerase chain reaction (PCR) on resulting cDNA were performed to determine relative expression of each gene of interest, determined by the C_T method and normalized to the relative expression of $18S$ or $ACTB$/β-actin. Sequences of primers are provided in table S4.

Quantification of SMAD phosphorylation in lung tissues

Lung samples were homogenized in radioimmunoprecipitation assay buffer [$1\times$ tris-buffered saline (TBS) with 1% NP-40, 0.5% sodium deoxycholate, and 0.1% SDS] supplemented with protease and phosphatase inhibitors (Thermo Fisher Scientific, 78442). Protein concentration was measured using Bradford assay (Thermo Fisher Scientific, 23236). Whole-lung extracts (30 μg) were separated by electrophoresis and Western blotting using specific antibodies recognizing p-Smad1/5/9 (Cell Signaling Technology, no. 9516), p-Smad2 (Cell Signaling Technology, no 3108), total Smad1 (Cell Signaling Technology, no. 6944), and glyceraldehyde-3-phosphate dehydrogenase (GAPDH) (Thermo Fisher Scientific, MA5–15738-HRP). Western blot was visualized using enhanced chemiluminescence.

Cell cultures

Human control PAECs (CC-2530), PMVECs (CC-2527), and PASMCs (CC-2581) were purchased from Lonza. TIME cells (CRL-4025) were purchased from ATCC and transfected with plasmid expressing firefly luciferase under the control of the BMP response element (BRE-Luc; provided by P. ten Dijke) using Lipofectamine 2000 (Thermo Fisher Scientific). PASMCs derived from PH and non-PH patient-derived cells were isolated from explanted pulmonary arterial tissues at the time of lung transplantation as previously described (45). PMVECs were obtained from PH and non-PH patients at the time of lung transplantation by tissue dissociation and magnetic bead separation as previously described (46). Demographic and clinical characteristics of the cell donors are described in table S5. PMVECs were

cultured in complete microvascular endothelial growth medium (EGM-2 MV) supplemented with 1% penicillin-streptomycin and 5% fetal calf serum (Lonza). Cell cultures were routinely tested for mycoplasma contamination and used only if negative and otherwise maintained as previously described (8).

Endothelial cell network formation assay

Control and PH patient-derived PMVECs were seeded into Geltrex Matrix (Thermo Fisher Scientific)–coated 24-well plates at 30,000 cells per well, in basal medium (EBM-2) containing 0.5% fetal bovine serum (FBS). Vehicle, ACTRIIA-Fc (2500 ng/ml), human VEGF (10 ng/ml), bFGF (10 ng/ml), BMP9 (1 ng/ml), GDF11 (100 ng/ml), GDF8 (100 ng/ml), activin A (100 ng/ml), or activin B (100 ng/ml) was added to basal medium. Separate wells were treated with endothelial basal growth media (EGM-2, Lonza) containing 2% FBS with or without ACTRIIA-Fc. After 13.5 hours of incubation at 37°C, cells were stained with calcein AM (2 μg/ml; Thermo Fisher Scientific) for 30 min at 37°C and imaged at 14 hours for green fluorescence at ×4 magnification. Images were taken at four quadrants of each well and analyzed using the ImageJ Angiogenesis Analyzer package version 1.52u to calculate the number and total length of branches (47).

Smooth muscle cell scratch migration assay

Control and PH patient-derived PASMCs were seeded in complete growth medium at 100,000 cells per well in 24-well plates. Once the cells reached confluence, they were starved overnight in smooth muscle cell basal growth medium (SmBM, Lonza) supplemented with 0.25% FBS. A scratch with a width of 1.5 mm was made along the midline of the well to remove cells. The wells were imaged along the midline at time 0 hours. The cells were treated in the basal medium with vehicle, ACTRIIA-Fc (2500 ng/ml), bFGF (10 ng/ml), GDF11 (100 ng/ml), GDF8 (100 ng/ml), activin A (100 ng/ml), activin B (100 ng/ml), or BMP4 (25 ng/ml) for 48 hours at 37°C. The cells were visualized using calcein AM (2 μg/ml, 0.5 hour, 37°C). The width of the cell-free streak was measured at 10 points per well at 0 and 48 hours. Cell migration was evaluated as average percentage reduction in the width using ImageJ.

Western blot analysis

Control and PH patient-derived cells were seeded in complete growth medium at 440,000 cells per well in 12-well plates. After overnight incubation, cells were starved in 0.5% FBS basal medium for 6 hours. Cells were pretreated with ACTRIIA-Fc (2500 ng/ml) for 30 min before being treated with GDF8 (50 ng/ml), GDF11 (50 ng/ml), activin A (50 ng/ml), activin B (50 ng/ml), BMP9 (100 pg/ml), TGFβ1 (1 ng/ml), or BMP 4 (50 ng/ml). After 30 min, wells were washed with PBS and harvested in 80 μl of 1× NuPAGE LDS Sample Buffer (Thermo Fisher Scientific, NP0007). Samples were incubated at 100°C for 5 min then separated by electrophoresis and Western blotting using specific antibodies recognizing phosphorylated forms of Smad1/3 (Abcam, 52903), Smad1/5/8 (Cell Signaling Technology, no. 9516), Smad2 (Cell Signaling Technology, no. 3108), total Smad1 (Cell Signaling Technology, no. 6944), and GAPDH (Thermo Fisher Scientific, MA5–15738-HRP). Western blot was detected with enhanced chemiluminescence.

In-Cell Western

Cell cultures were seeded onto 96-well plates, grown to confluence, deprived of serum for 6 hours (PMVECs) or 24 hours (all other cultures), and then incubated with various ligands. The plate was fixed with cold methanol, washed, and blocked with 2% bovine serum albumin in TBS. Primary antibodies specific for *p*-SMAD1/5 (Cell Signaling Technology, 9516) or *p*-SMAD2 (Cell Signaling Technology, 8828) were added (1:400 dilution), followed by secondary antibodies (HRP anti-rabbit IgG, Cell Signaling Technology; 1:1000). After washing, assays were developed using BioFX Chemiluminescent Ultra Sensitive HRP Microwell Substrate (Surmodics) and developed on a SpectraMax Plate Luminometer with 0.25-s integrations as previously described (48).

Thymidine proliferation assay

Control and PH patient-derived cells were seeded in complete growth medium at 25,000 cells per well in 96-well plates. After overnight incubation, cells were starved in basal media for 24 hours. After starvation, cells were pretreated with ACTRIIA-Fc (2500 ng/ml) for 30 min before being treated with GDF8 (50 ng/ml), GDF11 (50 ng/ml), activin A (50 ng/ml), activin B (50 ng/ml), BMP9 (100 pg/ml), or TGFβ1 (1 ng/ml) for 48 hours. Wells were treated with 1 μCi of ^{3}H-thymidine (PerkinElmer) for the last 6 hours of treatment incubation. Cells were washed with PBS and then trypsinized. Thymidine was harvested from each well and read using a 1450 MicroBeta TriLux microplate scintillation counter (PerkinElmer).

Apoptosis assay

Control and PH patient-derived cells were seeded in complete growth medium at 110,000 cells per well in an eight-well chamber slide. Once the cells reached confluence, they were treated with GDF11 (50 ng/ml), activin A (50 ng/ml), or BMP9 (100 pg/ml) in basal media for 48 hours. Cells were washed in PBS before 4% PFA fixation for 10 min at room temperature. Each well was then washed with PBS and stained with TUNEL stain (Trevigen, 4812–30-K) according to the kit protocol. This TUNEL staining kit was also used to stain paraffin-embedded lung sections according to the company's standard operating procedures.

Statistical analyses

Measurements and analysis of physiological parameters and vascular remodeling were performed in blinded fashion. Statistical analyses were performed using GraphPad Prism 8.4.0 and Stata 13.0 (StataCorp). The normality of all variables was tested using the Shapiro-Wilk test. Normally distributed variables are presented as means ± SEM, whereas non-normally distributed variables are presented as medians ± interquartile range. Normally distributed variables were compared using either Student's *t* test for two groups or one-way analysis of variance (ANOVA) with post hoc testing for multiple comparisons by Tukey's, Sidak's, Holm-Sidak's, or Dunnett's test for multiple comparisons, with a multiplicity adjusted $P < 0.05$ considered statistically significant. Non-normally distributed variables were compared using the Mann-Whitney test for two groups or the Kruskal-Wallis test followed by Dunn's multiple comparisons as indicated, with a multiplicity adjusted $P < 0.05$ considered statistically significant. Differences in proportions were analyzed by Fisher's

exact test or chi- square test as appropriate. In experiments testing the interaction of two treatments, two-way ANOVA was performed with Dunnett's test or Sidak's test for multiple comparisons indicated, as appropriate, with a multiplicity adjusted $P < 0.05$ considered statistically significant. All statistical tests were two sided.

Supplementary Material

Refer to Web version on PubMed Central for supplementary material.

REFERENCES AND NOTES

1. Simonneau G, Montani D, Celermajer DS, Denton CP, Gatzoulis MA, Krowka M, Williams PG, Souza R, Haemodynamic definitions and updated clinical classification of pulmonary hypertension. Eur. Respir. J 53, 1801913 (2019). [PubMed: 30545968]

2. Benza RL, Miller DP, Barst RJ, Badesch DB, Frost AE, McGoon MD, An evaluation of long-term survival from time of diagnosis in pulmonary arterial hypertension from the REVEAL Registry. Chest 142, 448–456 (2012). [PubMed: 22281797]

3. Soubrier F, Chung WK, Machado R, Grünig E, Aldred M, Geraci M, Loyd JE, Elliott CG, Trembath RC, Newman JH, Humbert M, Genetics and genomics of pulmonary arterial hypertension. J. Am. Coll. Cardiol 62, D13–D21 (2013). [PubMed: 24355637]

4. Gräf S, Haimel M, Bleda M, Hadinnapola C, Southgate L, Li W, Hodgson J, Liu B, Salmon RM, Southwood M, Machado RD, Martin JM, Treacy CM, Yates K, Daugherty LC, Shamardina O, Whitehorn D, Holden S, Aldred M, Bogaard HJ, Church C, Coghlan G, Condliffe R, Corris PA, Danesino C, Eyries M, Gall H, Ghio S, Ghofrani H-A, Gibbs JSR, Girerd B, Houweling AC, Howard L, Humbert M, Kiely DG, Kovacs G, MacKenzie Ross RV, Moledina S, Montani D, Newnham M, Olschewski A, Olschewski H, Peacock AJ, Pepke-Zaba J, Prokopenko I, Rhodes CJ, Scelsi L, Seeger W, Soubrier F, Stein DF, Suntharalingam J, Swietlik EM, Toshner MR, van Heel DA, Noordegraaf AV, Waisfisz Q, Wharton J, Wort SJ, Ouwehand WH, Soranzo N, Lawrie A, Upton PD, Wilkins MR, Trembath RC, Morrell NW, Identification of rare sequence variation underlying heritable pulmonary arterial hypertension. Nat. Commun 9, 1416 (2018). [PubMed: 29650961]

5. Thomas M, Docx C, Holmes AM, Beach S, Duggan N, England K, Leblanc C, Lebret C, Schindler F, Raza F, Walker C, Crosby A, Davies RJ, Morrell NW, Budd DC, Activin-like kinase 5 (ALK5) mediates abnormal proliferation of vascular smooth muscle cells from patients with familial pulmonary arterial hypertension and is involved in the progression of experimental pulmonary arterial hypertension induced by monocrotaline. Am. J. Pathol 174, 380–389 (2009). [PubMed: 19116361]

6. Wang G, Fan R, Ji R, Zou W, Penny DJ, Varghese NP, Fan Y, Novel homozygous BMP9 nonsense mutation causes pulmonary arterial hypertension: A case report. BMC Pulm. Med 16, 17 (2016). [PubMed: 26801773]

7. Upton PD, Davies RJ, Trembath RC, Morrell NW, Bone morphogenetic protein (BMP) and activin type II receptors balance BMP9 signals mediated by activin receptor-like kinase-1 in human pulmonary artery endothelial cells. J. Biol. Chem 284, 15794–15804 (2009). [PubMed: 19366699]

8. Yung L-M, Nikolic I, Paskin-Flerlage SD, Pearsall RS, Kumar R, Yu PB, A selective transforming growth factor-β ligand trap attenuates pulmonary hypertension. Am. J. Respir. Crit. Care Med 194, 1140–1151 (2016). [PubMed: 27115515]

9. Botney MD, Bahadori L, Gold LI, Vascular remodeling in primary pulmonary hypertension. Potential role for transforming growth factor-beta. Am. J. Pathol 144, 286–295 (1994). [PubMed: 8311113]

10. Long L, Ormiston ML, Yang X, Southwood M, Gräf S, Machado RD, Mueller M, Kinzel B, Yung LM, Wilkinson JM, Moore SD, Drake KM, Aldred MA, Yu PB, Upton PD, Morrell NW, Selective enhancement of endothelial BMPR-II with BMP9 reverses pulmonary arterial hypertension. Nat. Med 21, 777–785 (2015). [PubMed: 26076038]

11. Nikolic I, Yung L-M, Yang P, Malhotra R, Paskin-Flerlage SD, Dinter T, Bocobo GA, Tumelty KE, Faugno AJ, Troncone L, McNeil ME, Huang X, Coser KR, Lai CSC, Upton PD, Goumans MJ, Zamanian RT, Elliott CG, Lee A, Zheng W, Berasi SP, Huard C, Morrell NW, Chung RT, Channick RW, Roberts KE, Yu PB, Bone morphogenetic protein 9 is a mechanistic biomarker of portopulmonary hypertension. Am. J. Respir. Crit. Care Med 199, 891–902 (2019). [PubMed: 30312106]

12. Zaiman AL, Podowski M, Medicherla S, Gordy K, Xu F, Zhen L, Shimoda LA, Neptune E, Higgins L, Murphy A, Chakravarty S, Protter A, Sehgal PB, Champion HC, Tuder RM, Role of the TGF-β/Alk5 signaling pathway in monocrotaline-induced pulmonary hypertension. Am. J. Respir. Crit. Care Med 177, 896–905 (2008). [PubMed: 18202349]

13. Chen Y-F, Feng J-A, Li P, Xing D, Zhang Y, Serra R, Ambalavanan N, Majid-Hassan E, Oparil S, Dominant negative mutation of the TGF-β receptor blocks hypoxia-induced pulmonary vascular remodeling. J. Appl. Physiol 100, 564–571 (2006). [PubMed: 16223981]

14. Sheares KK, Jeffery TK, Long L, Yang X, Morrell NW, Differential effects of TGF-β1 and BMP-4 on the hypoxic induction of cyclooxygenase-2 in human pulmonary artery smooth muscle cells. Am. J. Physiol. Lung Cell. Mol. Physiol 287, L919–L927 (2004). [PubMed: 15220111]

15. Graham BB, Chabon J, Gebreab L, Poole J, Debella E, Davis L, Tanaka T, Sanders L, Dropcho A. Bandeira, Vandivier RW, Champion HC, Butrous G, Wang X-J, Wynn TA, Tuder RM, Transforming growth factor-β signaling promotes pulmonary hypertension caused by Schistosoma mansoni. Circulation 128, 1354–1364 (2013). [PubMed: 23958565]

16. Yan Y, Wang X-J, Li S-Q, Yang S-H, Lv Z-C, Wang L-T, He Y-Y, Jiang X, Wang Y, Jing Z-C, Elevated levels of plasma transforming growth factor-β1 in idiopathic and heritable pulmonary arterial hypertension. Int. J. Cardiol 222, 368–374 (2016). [PubMed: 27500766]

17. Long L, Crosby A, Yang X, Southwood M, Upton PD, Kim D-K, Morrell NW, Altered bone morphogenetic protein and transforming growth factor-β signaling in rat models of pulmonary hypertension: Potential for activin receptor-like kinase-5 inhibition in prevention and progression of disease. Circulation 119, 566–576 (2009). [PubMed: 19153267]

18. Yndestad A, Larsen K-O, Øie E, Ueland T, Smith C, Halvorsen B, Sjaastad I, Skjønsberg H, Pedersen TM, Anfinsen O-G, Damås JK, Christensen G, Aukrust P, Andreassen AK, Elevated levels of activin A in clinical and experimental pulmonary hypertension. J. Appl. Physiol 106, 1356–1364 (2009). [PubMed: 19196915]

19. Kudryashova TV, Shen Y, Pena A, Cronin E, Okorie E, Goncharov DA, Goncharova EA, Inhibitory antibodies against activin A and TGF-β reduce self-supported, but not soluble factors-induced growth of human pulmonary arterial vascular smooth muscle cells in pulmonary arterial hypertension. Int. J. Mol. Sci 19, E2957 (2018). [PubMed: 30274147]

20. Sun N, Chen Y, Yu F, Zhixin F, Lin J, Sun B, Yu B, Cheng X, Zheng X, Wu B, Monocrotaline pyrrole enhanced bone morphogenetic protein 7 signaling transduced by alternative activin A receptor type 2A in pulmonary arterial smooth muscle cells. Eur. J. Pharmacol 863, 172679 (2019). [PubMed: 31542483]

21. Komrokji R, Garcia-Manero G, Ades L, Prebet T, Steensma DP, Jurcic JG, Sekeres MA, Berdeja J, Savona MR, Beyne-Rauzy O, Stamatoullas A, DeZern AE, Delaunay J, Borthakur G, Rifkin R, Boyd TE, Laadem A, Vo B, Zhang J, Puccio-Pick M, Attie KM, Fenaux P, List AF, Sotatercept with long-term extension for the treatment of anaemia in patients with lower-risk myelodysplastic syndromes: A phase 2, dose-ranging trial. Lancet Haematol. 5, e63–e72 (2018). [PubMed: 29331635]

22. Raje N, Vallet S, Sotatercept, a soluble activin receptor type 2A IgG-Fc fusion protein for the treatment of anemia and bone loss. Curr. Opin. Mol. Ther 12, 586–597 (2010). [PubMed: 20886391]

23. Abe K, Toba M, Alzoubi A, Ito M, Fagan KA, Cool CD, Voelkel NF, McMurtry IF, Oka M, Formation of plexiform lesions in experimental severe pulmonary arterial hypertension. Circulation 121, 2747–2754 (2010). [PubMed: 20547927]

24. Schermuly RT, Dony E, Ghofrani HA, Pullamsetti S, Savai R, Roth M, Sydykov A, Lai YJ, Weissmann N, Seeger W, Grimminger F, Reversal of experimental pulmonary hypertension by PDGF inhibition. J. Clin. Invest 115, 2811–2821 (2005). [PubMed: 16200212]

25. Hoeper MM, Barst RJ, Bourge RC, Feldman J, Frost AE, Galié N, Gómez-Sánchez MA, Grimminger F, Grunig E, Hassoun PM, Morrell NW, Peacock AJ, Satoh T, Simonneau G, Tapson VF, Torres F, Lawrence D, Quinn DA, Ghofrani HA, Imatinib mesylate as add-on therapy for pulmonary arterial hypertension: Results of the randomized IMPRES study. Circulation 127, 1128–1138 (2013). [PubMed: 23403476]

26. Ghofrani HA, Seeger W, Grimminger F, Imatinib for the treatment of pulmonary arterial hypertension. N. Engl. J. Med 353, 1412–1413 (2005). [PubMed: 16192491]

27. David L, Mallet C, Mazerbourg S, Feige JJ, Bailly S, Identification of BMP9 and BMP10 as functional activators of the orphan activin receptor-like kinase 1 (ALK1) in endothelial cells. Blood 109, 1953–1961 (2007). [PubMed: 17068149]

28. Townson SA, Martinez-Hackert E, Greppi C, Lowden P, Sako D, Liu J, Ucran JA, Liharska K, Underwood KW, Seehra J, Kumar R, Grinberg AV, Specificity and structure of a high affinity activin receptor-like kinase 1 (ALK1) signaling complex. J. Biol. Chem 287, 27313–27325 (2012). [PubMed: 22718755]

29. Yu PB, Deng DY, Beppu H, Hong CC, Lai C, Hoyng SA, Kawai N, Bloch KD, Bone morphogenetic protein (BMP) type II receptor is required for BMP-mediated growth arrest and differentiation in pulmonary artery smooth muscle cells. J. Biol. Chem 283, 3877–3888 (2008). [PubMed: 18042551]

30. Yu PB, Beppu H, Kawai N, Li E, Bloch KD, Bone morphogenetic protein (BMP) type II receptor deletion reveals BMP ligand-specific gain of signaling in pulmonary artery smooth muscle cells. J. Biol. Chem 280, 24443–24450 (2005). [PubMed: 15883158]

31. Olsen OE, Wader KF, Hella H, Mylin AK, Turesson I, Nesthus I, Waage A, Sundan A, Holien T, Activin A inhibits BMP-signaling by binding ACVR2A and ACVR2B. Cell Commun. Signal 13, 27 (2015). [PubMed: 26047946]

32. Yu X, Chen X, Zheng XD, Zhang J, Zhao X, Liu Y, Zhang H, Zhang L, Yu H, Zhang M, Ma C, Hao X, Zhu D, Growth differentiation factor 11 promotes abnormal proliferation and angiogenesis of pulmonary artery endothelial cells. Hypertension 71, 729–741 (2018). [PubMed: 29463625]

33. Walker RG, Czepnik M, Goebel EJ, McCoy JC, Vujic A, Cho M, Oh J, Aykul S, Walton KL, Schang G, Bernard DJ, Hinck AP, Harrison CA, Martinez-Hackert E, Wagers AJ, Lee RT, Thompson TB, Structural basis for potency differences between GDF8 and GDF11. BMC Biol. 15, 19 (2017). [PubMed: 28257634]

34. McPherron AC, Huynh TV, Lee S-J, Redundancy of myostatin and growth/ differentiation factor 11 function. BMC Dev. Biol 9, 24 (2009). [PubMed: 19298661]

35. Latres E, Mastaitis J, Fury W, Miloscio L, Trejos J, Pangilinan J, Okamoto H, Cavino K, Na E, Papatheodorou A, Willer T, Bai Y, Hae Kim J, Rafique A, Jaspers S, Stitt T, Murphy AJ, Yancopoulos GD, Gromada J, Activin A more prominently regulates muscle mass in primates than does GDF8. Nat. Commun 8, 15153 (2017). [PubMed: 28452368]

36. Bayarsaikhan O, Kawai N, Mori H, Kinouchi N, Nikawa T, Tanaka E, Co-Administration of myostatin-targeting siRNA and ActRIIB-Fc fusion protein increases masseter muscle mass and fiber size. J. Nutr. Sci. Vitaminol 63, 244–248 (2017). [PubMed: 28978871]

37. Amthor H, Hoogaars WM, Interference with myostatin/ActRIIB signaling as a therapeutic strategy for Duchenne muscular dystrophy. Curr. Gene Ther 12, 245–259 (2012). [PubMed: 22554312]

38. George Carlson C, Bruemmer K, Sesti J, Stefanski C, Curtis H, Ucran J, Lachey J, Seehra JS, Soluble activin receptor type IIB increases forward pulling tension in the mdx mouse. Muscle Nerve 43, 694–699 (2011). [PubMed: 21462203]

39. Abdulkadyrov KM, Salogub GN, Khuazheva NK, Sherman ML, Laadem A, Barger R, Knight R, Srinivasan S, Terpos E, Sotatercept in patients with osteolytic lesions of multiple myeloma. Br. J. Haematol 165, 814–823 (2014). [PubMed: 24650009]

40. Dussiot M, Maciel TT, Fricot A, Chartier C, Negre O, Veiga J, Grapton D, Paubelle E, Payen E, Beuzard Y, Leboulch P, Ribeil J-A, Arlet J-B, Coté F, Courtois G, Ginzburg YZ, Daniel TO, Chopra R, Sung V, Hermine O, Moura IC, An activin receptor IIA ligand trap corrects ineffective erythropoiesis in β-thalassemia. Nat. Med 20, 398–407 (2014). [PubMed: 24658077]

41. Sherman ML, Borgstein NG, Mook L, Wilson D, Yang Y, Chen N, Kumar R, Kim K, Laadem A, Multiple-dose, safety, pharmacokinetic, and pharmacodynamic study of sotatercept (ActRIIA-IgG1), a novel erythropoietic agent, in healthy postmenopausal women. J. Clin. Pharmacol 53, 1121–1130 (2013). [PubMed: 23939631]

42. Ulrich A, Wharton J, Thayer TE, Swietlik EM, Assad TR, Desai AA, Gräf S, Harbaum L, Humbert M, Morrell NW, Nichols WC, Soubrier F, Southgate L, Trégouët DA, Trembath RC, Brittain EL, Wilkins MR, Prokopenko I, Rhodes CJ; NIHR BioResource – Rare Diseases Consortium; UK PAH Cohort Study Consortium; US PAH Biobank Consortium, Mendelian randomisation analysis of red cell distribution width in pulmonary arterial hypertension. Eur. Respir. J 55, 1901486 (2020). [PubMed: 31744833]

43. Rhodes CJ, Wharton J, Howard L, Gibbs JS, Vonk-Noordegraaf A, Wilkins MR, Iron deficiency in pulmonary arterial hypertension: A potential therapeutic target. Eur. Respir. J 38, 1453–1460 (2011). [PubMed: 21478213]

44. Pearsall RS, Canalis E, Cornwall-Brady M, Underwood KW, Haigis B, Ucran J, Kumar R, Pobre E, Grinberg A, Werner ED, Glatt V, Stadmeyer L, Smith D, Seehra J, Bouxsein ML, A soluble activin type IIA receptor induces bone formation and improves skeletal integrity. Proc. Natl. Acad. Sci. U.S.A 105, 7082–7087 (2008). [PubMed: 18460605]

45. Comhair SA, Xu W, Mavrakis L, Aldred MA, Asosingh K, Erzurum SC, Human primary lung endothelial cells in culture. Am. J. Respir. Cell Mol. Biol 46, 723–730 (2012). [PubMed: 22427538]

46. Szulcek R, Happé CM, Rol N, Fontijn RD, Dickhoff C, Hartemink KJ, Grunberg K, Tu L, Timens W, Nossent GD, Paul MA, Leyen TA, Horrevoets AJ, de Man FS, Guignabert C, Yu PB, Vonk-Noordegraaf A, van Nieuw Amerongen GP, Bogaard HJ, Delayed microvascular shear adaptation in pulmonary arterial hypertension. Role of platelet endothelial cell adhesion molecule-1 cleavage. Am. J. Respir. Crit. Care Med 193, 1410–1420 (2016). [PubMed: 26760925]

47. Carpentier G, Description of Angiogenesis Analyzer Package. (NIH, 2020), vol. 2020.

48. Dinter T, Bocobo GA, Yu PB, Pharmacologic strategies for assaying BMP signaling function. Methods Mol. Biol 1891, 221–233 (2019). [PubMed: 30414136]
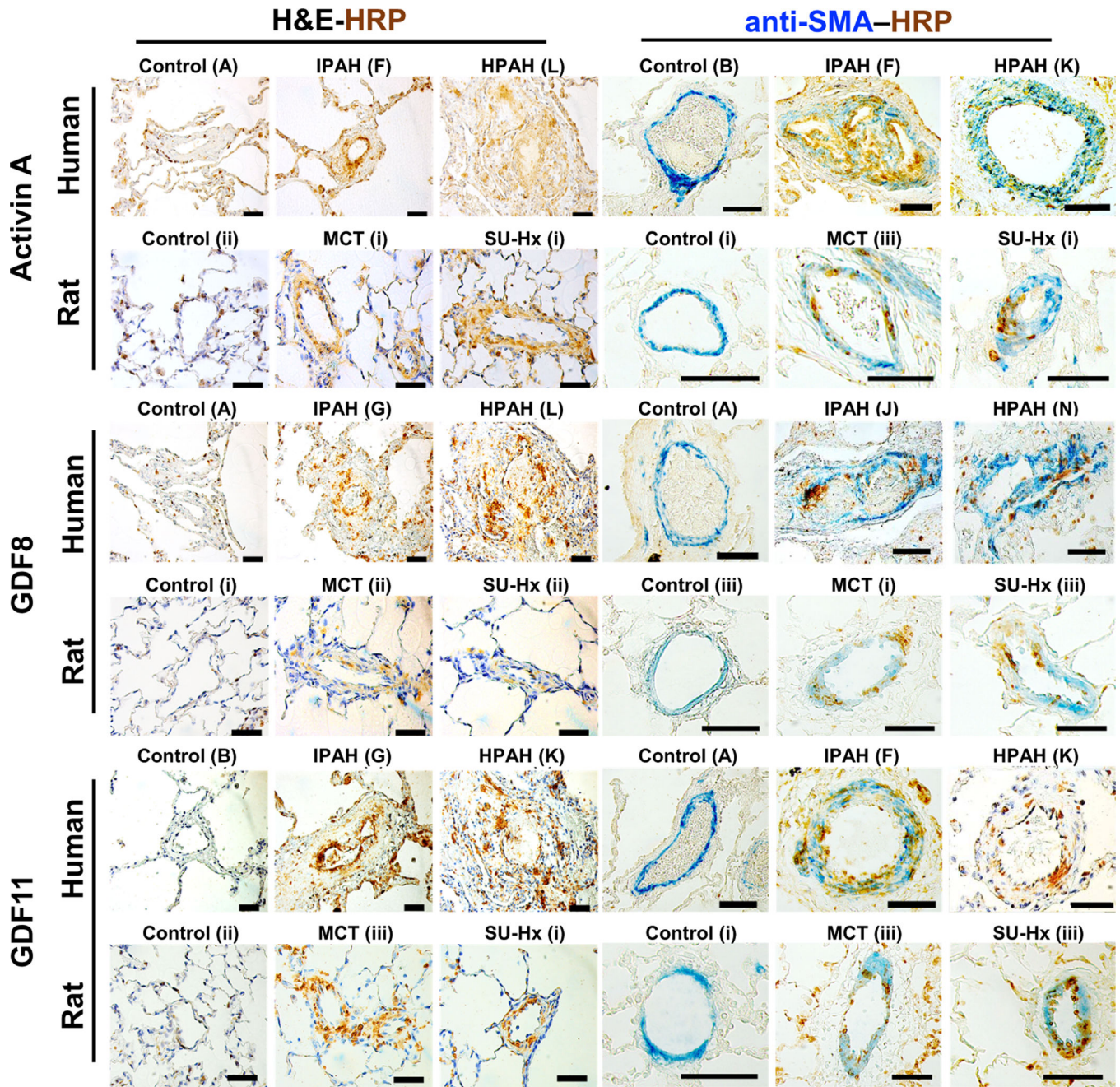
Fig. 1. ACTRIIA ligands activin A, GDF8, and GDF11 are expressed in the intima and media of small arterioles in human PAH and rat PH.

Immunohistochemical staining for activin A, GDF8, and GDF11 along with α-SMA costain performed on paraffin-embedded lung sections from healthy controls and patients with IPAH or HPAH ($n = 5$ each) and lung sections from control, MCT-exposed, or SU-Hx–exposed rats ($n = 3$ each). Horseradish peroxidase (HRP)–conjugated secondary antibody (3,3′-diaminobenzidine staining, as indicated by label HRP in brown) and α-smooth muscle actin (α-SMA) AP-conjugated primary antibody (as indicated by label SMA in blue; right) are shown. Scale bars, 50 μm.
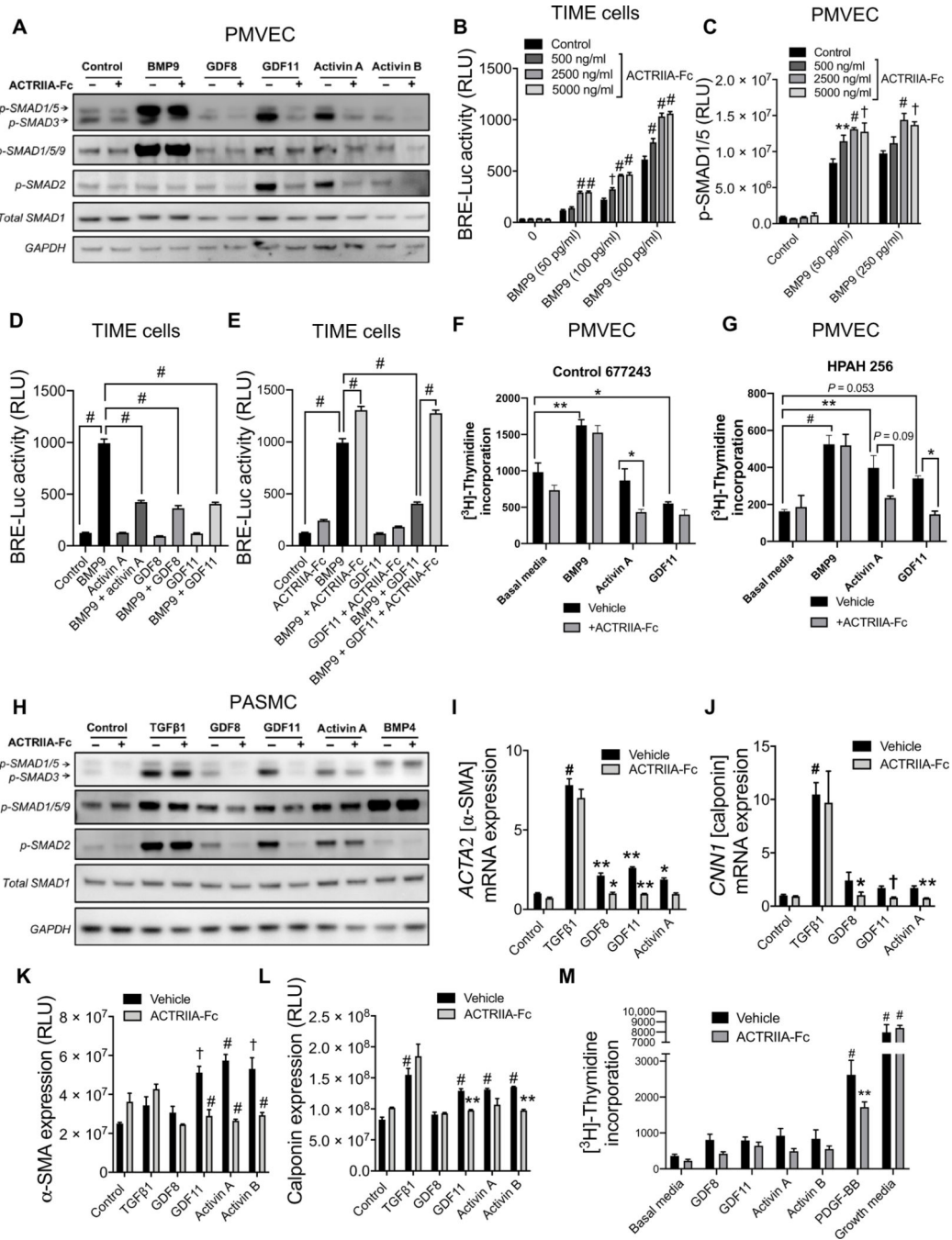
Fig. 2. ACTRIIA-Fc modulates signaling, gene regulation, and proliferation of human pulmonary vascular cells.

(**A**) Expression of phosphorylated SMAD1/5/9 and SMAD2/3 in human pulmonary micro-vascular endothelial cells (PMVECs) exposed to BMP9 (100 pg/ml), GDF8 (50 ng/ml), GDF11 (50 ng/ml), activin A (50 ng/ml), or activin B (50 ng/ ml) for 30 min with or without ACTRIIA-Fc (2500 ng/ml), analyzed by Western blot. $n = 3$ replicates; $N = 3$ independent experiments. (**B**) Luciferase activity in telomerase immortalized human microvascular endothelial (TIME) cells transfected with BMP-responsive element transcriptional reporter

(*BRE-Luc*) and exposed to varying concentrations of BMP9 with or without ACTRIIA-Fc ($n = 3$; $N = 3$; RLU, relative luminescence units). (**C**) Activation of SMAD1/5 in human PMVECs treated with BMP9 (below the EC_{50} 250 ng/ml) with or without varying concentrations of ACTRIIA-Fc, analyzed by In-Cell Western. Data represent means ± SEM. *$P < 0.05$, **$P < 0.01$, †$P < 0.001$, and #$P < 0.0001$ compared to untreated controls in each group, two-way ANOVA with Dunnett's test for multiple comparisons ($n = 3$; $N = 3$). (**D** and **E**) BMP-mediated transcriptional activity in TIME cells treated with BMP9, GDF8, GDF11, and activin A with or without ACTRIIA-Fc ($n = 6$; $N = 3$). (**F** and **G**) Proliferation of control- and PAH-derived PMVECs in response to BMP9, activin A, and GDF11 with or without ACTRIIA-Fc. (**H**) Expression of phosphorylated SMAD1/5/9 and SMAD2/3 in human pulmonary artery smooth muscle cells (PASMCs) exposed to TGFβ1 (1 ng/ml), GDF8 (50 ng/ml), GDF11 (50 ng/ml), activin A (50 ng/ml), or BMP4 (50 ng/ml) for 30 min with or without ACTRIIA-Fc (2500 ng/ml), analyzed by Western blot. (**I** and **J**) Expression of α-SMA and calponin mRNA at 24 hours after stimulation with TGFβ1 (1 ng/ml), GDF8 (50 ng/ml), GDF11 (50 ng/ml), or activin A (50 ng/ml) in human PASMCs with or without ACTRIIA-Fc ($n = 3$ to 6). (**K** and **L**) Expression of α-SMA and calponin protein in PASMCs at 72 hours after stimulation with TGFβ1, GDF8, GDF11, activin A, or activin B with or without ACTRIIA-Fc, as assessed by In-Cell Western ($n = 4$; $N = 3$). (**M**) Proliferation in PASMCs exposed to GDF8 (100 ng/ml), GDF11 (100 ng/ml), activin A (100 ng/ml), activin B (100 ng/ml), PDGF-BB (1 ng/ml), or complete media for 24 hours with or without ACTRIIA-Fc (10,000 ng/ml) as measured by ^{3}H-thymidine incorporation. ($n = 5$; $N = 3$). Data represent means ± SEM. *$P < 0.05$, **$P < 0.01$, †$P < 0.001$, and #$P < 0.0001$ compared to vehicle controls, one-way ANOVA with Sidak's test for multiple comparisons.
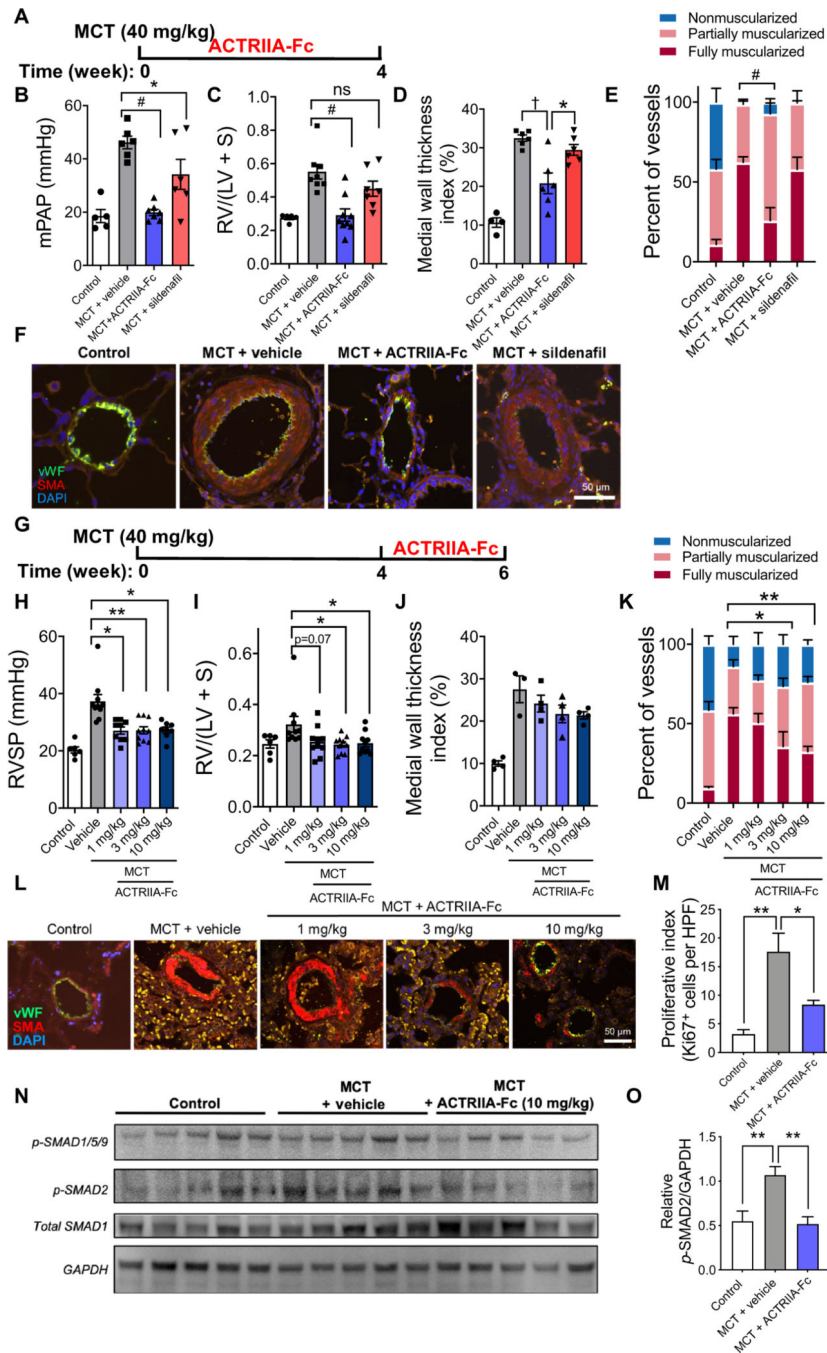
Fig. 3. ACTRIIA-Fc attenuates PH and vascular remodeling in MCT-exposed rats.
(**A**) Treatment timing of adult rats after vehicle or MCT (40 mg/ kg, sc) with ACTRIIA-Fc (15 mg/kg, ip, twice weekly), sildenafil [30 mg/kg, orally, twice daily], or vehicle (10 mM TBS) for 4 weeks starting 1 day after MCT. (**B**) Mean pulmonary artery pressure (mPAP) and (**C**) RV hypertrophy (RVH) in rats treated with ACTRIIA-Fc or sildenafil compared to vehicle (n = 5 to 9 per group). Data represent means ± SEM. *$P < 0.05$, **$P < 0.01$, #$P < 0.0001$, and not significant (ns; $P > 0.05$) as indicated, one-way ANOVA with Sidak's post test for mPAP and Kruskal-Wallis test with Dunn's post test for RVH. (**D**) Medial wall

thickness index and (**E**) the percentage of fully muscularized vessels in rats treated with ACTRIIA-Fc or sildenafil compared to vehicle (diameter, 10 to 50 μm). Values are shown as means ± SEM. $n = 3$ to 6 per group (30 to 50 vessels counted per sample). *$P < 0.05$, **$P < 0.01$, †$P < 0.001$, and #$P < 0.0001$ as indicated, one-way and two-way ANOVA with Tukey's and Dunnett's test for multiple comparisons. (**F**) Immunofluorescence images of pulmonary arteriole medial hypertrophy in lung sections from rats with MCT-induced PH treated with vehicle, ACTRIIA-Fc, or sildenafil. vWF, von Willebrand factor; SMA, α-SMA; DAPI, 4′,6-diamidino-2-phenylindole (nuclear stain). (**G**) Treatment timing of rats with established PH, with ACTRIIA-Fc (1, 3, and 10 mg/kg, ip, twice weekly) or isotype control with vehicle (mIgG2a, 10 mg/kg, ip, twice weekly) starting on day 28 after MCT. (**H**) RV systolic pressure (RVSP) and (**I**) RVH in rats treated with control IgG or ACTRIIA-Fc measured among surviving animals at 42 days ($n = 6$ to 10 per group). Values are shown as means ± SEM. *$P < 0.05$ and **$P < 0.01$, Kruskal-Wallis test with Dunn's post test for multiple comparisons. (**J**) Medial wall thickness and (**K**) percentage of muscularized vessels in rats with established PH treated with vehicle IgG or ACTRIIA-Fc compared to control. Values are shown as means ± SEM. $n = 3$ to 6 per group (30 to 50 vessels counted per sample). *$P < 0.05$, **$P < 0.01$, †$P < 0.001$, and #$P < 0.0001$ as indicated, two-way ANOVA with Dunnett's test for multiple comparisons. (**L**) Immunofluorescence images of MCT-induced medial hypertrophy in pulmonary arterioles from rats with established PH treated with vehicle IgG or ACTRIIA-Fc. (**M**) Ki67-positive cells in MCT-PH lungs treated with vehicle IgG or ACTRIIA-Fc. Values are shown as means ± SEM. $n = 3$ to 6 per group [20 random high-powered fields (HPF) containing >30 to 50 vessels counted per sample]. (**N**) Western blot and (**O**) densitometric analysis of phosphorylation of SMAD2 in lung lysates from MCT-exposed rats treated with vehicle IgG or ACTRIIA-Fc in comparison to control rats. Data represent means ± SEM. $n = 3$ to 4. *$P < 0.05$ and **$P < 0.01$, one-way ANOVA with Tukey's test for multiple comparisons. Scale bars, 50 μm.
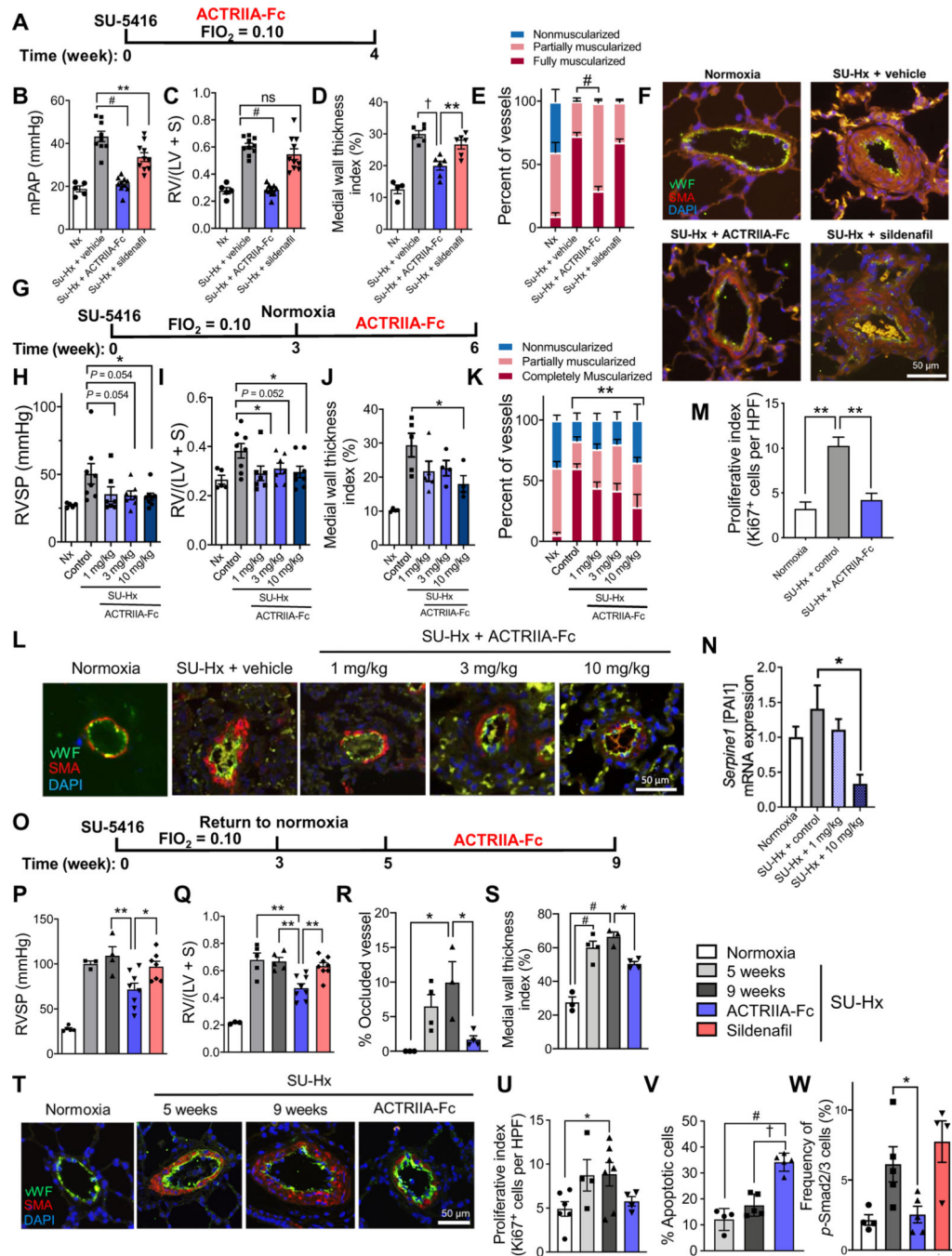
Fig. 4. ACTRIIA-Fc ameliorates PH and vascular remodeling in SU-Hx–exposed rats.
(**A**) Treatment timing for SU-Hx PH. Male adult rats were injected with vehicle or
VEGFR1/2 inhibitor SUGEN5416 (200 mg/kg, sc), subjected to normoxia (Nx) or
normobaric hypoxia (FiO$_2$ = 0.10) for 4 weeks, and received ACTRIIA-Fc (10 mg/kg, ip,
twice weekly), sildenafil (60 mg/kg, twice daily, orally), or vehicle (10 mM TBS) for 4
weeks starting 1 day after SUGEN5416. (**B**) mPAP and (**C**) RVH in Nx-exposed and SU-
Hx–exposed rats treated with ACTRIIA-Fc or sildenafil as compared to TBS vehicle–treated
rats (n = 5 to 10 per group). Values are shown as means ± SEM. **P< 0.01 and #P<

0.0001, as indicated, one-way ANOVA with Dunnett's multiple comparisons test. (**D**) Medial wall thickness and (**E**) the percentage of muscularized vessels (diameter, 10 to 50 μm) in rats treated with sildenafil or ACTRIIA-Fc as in (B). Values are shown as means ± SEM. n = 4 to 6 per group (30 to 50 vessels counted per sample). *P < 0.05, **P < 0.01, †P < 0.001, and #P < 0.0001 as indicated, one-way or two-way ANOVA with Tukey's or Dunnett's test for multiple comparisons. (**F**) Immunofluorescence images of medial hypertrophy of pulmonary arterioles in Nx-exposed and SU-Hx–exposed rats treated with vehicle, ACTRIIA-Fc, or sildenafil. (**G**) Treatment timing for established PH in SU-Hx model. Male adult rats received a single injection of SUGEN5416 (20 mg/kg, sc) and were subjected to normobaric hypoxia (FiO$_2$ = 0.10) for 3 weeks, followed by 3 weeks of normoxia during which rats received varying doses of ACTRIIA-Fc (1, 3, or 10 mg/kg, ip, twice weekly) or isotype control (mIgG2a; 10 mg/kg, ip, twice weekly). (**H**) RVSP and (**I**) RVH in rats treated as in (G) (n = 5 to 8 per group). *P < 0.05, one-way ANOVA with Holm- Sidak's test for multiple comparisons. (**J** and **K**) The highest dose of ACTRIIA-Fc attenuated medial wall thickening and (K) the percent-* age of muscularized vessels in rats treated as in (G). *P < 0.05 and **P < 0.01 as indicated, one-way and two-way ANOVA with Tukey's and Dunnett's tests for multiple comparisons. Values are shown as means ± SEM. n = 4 to 8 per group (30 to 50 vessels counted per sample). (**L**) Immunofluorescence images of medial hypertrophy and neointimal lesion formation in pulmonary arterioles from rats treated as in (G). (**M**) Quantification of proliferation index in small vessels and perivascular tissues of SU-Hx rats treated with isotype control or high dose of ACTRIIA-Fc. **P < 0.01, one-way ANOVA with Tukey's test for multiple comparisons. Values are shown as means ± SEM. n = 3 to 4 per group (20 random high-powered fields of view quantified per sample). (**N**) *Pai-1* mRNA expression via quantitative RT-PCR in lung tissues from rats with SU-Hx treated with ACTRIIA-Fc or control. *P < 0.05, one-way ANOVA with Tukey's test for multiple comparisons. Values are shown as means ± SEM. n = 3 to 4 per group. (**O**) Treatment timing for rats with severe obliterative PH. SU-Hx rats were allowed to progress for 2 weeks under normoxia after 3 weeks of SU-Hx (20 mg/kg, sc; FiO$_2$ = 0.10), followed by 4 weeks of treatment with vehicle, ACTRIIA-Fc, or sildenafil. (**P**) RVSP and (**Q**) RVH in untreated rats after 5 and 9 weeks or rats treated with ACTRIIA-Fc or sildenafil from weeks 6 to 9 (n = 3 to 8). *P < 0.05 and **P < 0.01, one-way ANOVA with Tukey's test for multiple comparisons. (**R**) Proportion of occluded vessels (n = 3 to 4) and (**S**) vascular wall thickness index (n = 3 to 4 and 30 to 50 vessels counted per sample) in rats as in (P). (**T**) Immunofluorescence images of intimal and medial remodeling in pulmonary arterioles in SU-Hx rats with or without ACTRIIA-Fc treatment. (**U**) Proliferative index in small vessels and perivascular tissues in SU-Hx rats with or without ACTRIIA-Fc (P = 0.19 ACTRIIA-Fc compared to week 9, n = 4 to 6, 20 random high-powered fields of view quantified per sample). (**V**) Percentage of apoptotic vascular cells (TUNEL$^+$ vessel-associated cells) in ACTRIIA-Fc–treated rats as compared to untreated rats at 5 and 9 weeks after SU-Hx treatment (n = 4 to 6). (**W**) Percentage of p-SMAD2/3$^+$ cells in the luminal wall and media of remodeled vessels in ACTRIIA-Fc–, sildenafil-, or vehicle-treated SU-Hx rats at 9 weeks (n = 4 to 5). Values for (P) to (W) are shown as means ± SEM. *P < 0.05, **P < 0.01, †P < 0.001, and #P < 0.0001 as indicated, one-way ANOVA with Tukey's test for multiple comparisons. Scale bars, 50 μm.